Ecological Complexity 21 (2015) 14–26

Contents lists available at ScienceDirect

Ecological Complexity

journal homepage: www.elsevier.com/locate/ecocom

Original Research Article

Understanding the interplay between density dependent birth function and maturation time delay using a reaction-diffusion population model

Majid Bani-Yaghoub [a,*], Guangming Yao [b], Masami Fujiwara [c], David E. Amundsen [d]

[a] Department of Mathematics and Statistics, University of Missouri-Kansas City, Kansas City, MO, 64110-2499, USA
[b] Department of Mathematics, Clarkson University, Potsdam, NY, 13699-5815, USA
[c] Department of Wildlife and Fisheries Sciences, Texas A&M University, TAMU 2258, College Station, TX 77843-2258, USA
[d] School of Mathematics and Statistics, Carleton University, ON K1S-5B6, Canada

ARTICLE INFO

Article history:
Received 13 November 2013
Received in revised form 22 October 2014
Accepted 23 October 2014
Available online 28 November 2014

Keywords:
Delay
Extinction
Reaction-diffusion
Single species
Allee effect

ABSTRACT

The present work employs a nonlocal delay reaction-diffusion model to study the impacts of the density dependent birth function, maturation time delay and population dispersal on single species dynamics (i.e., extinction, survival, extinction-survival). It is shown that the maturation time and the birth function are two major factors determining the fate of single species. Whereas the dispersal acts as a subsidiary factor that only affects the spatial patterns of population densities. When the birth function has a compensating density dependence, maturation time delay cannot destabilize the population survival at the positive equilibrium. Nevertheless, when the birth function has an over-compensating density dependence, the population densities of single species fluctuate in the spatial domain due to the increased maturation time delay. With the Allee effect and over-compensating density dependence, the increases in the maturation time may cause extinction of the single species in the entire spatial domain. The numerical simulations suggest that the solutions of the general model may temporarily remain nearby a stationary wave pulse or a stationary wavefront of the reduced model. The former indicates the survival of single species in a narrow region of the spatial domain. Whereas the latter represents the survival in the entire left-half or right-half of the spatial domain.

1. Introduction

Mathematical models in population biology and epidemiology are becoming more sophisticated and therefore more challenging. In the last two decades, there has been a significant progress in mathematical modeling of spatially structured populations. Two contemporary modeling approaches that have been the center of attention are known as Britton's and Smith-Thieme approaches. Namely, the Britton's approach Britton (1989, 1990) takes into account the aggregation mechanism of the population through a spatio-temporal convolution, whereas the Smith-Thieme approach Smith and Thieme (1991) incorporates age structures into the population models. Employing either of these approaches, various nonlocal delay diffusive models have been proposed Gourley et al. (2004), Liang et al. (2005), Weng et al. (2008). Analyses of these models are mainly focused on the existence and behavior of traveling wave solutions Gourley et al. (2004), Liang and Wu (2003), So et al. (2001). Nonetheless, there is a need to compare the possible outcomes of the new models with those of the traditional models. Specifically, the spatio-temporal patterns resulting from the new models may reveal population dynamics and crucial factors that have been overlooked by the traditional models.

In the present work we study the possible outcomes of the general age-structured population model proposed by So et al. (2001). The model has been developed using the Smith-Thieme approach for one-dimensional unbounded domain. In particular, let $u(x, a, t)$ denote the population density of the single species at time $t \geq 0$, age $a \geq 0$, and location $x \in (-\infty, \infty)$. Then the authors start with the following age-structured model proposed in Metz and Diekmann (1986).

$$\frac{\partial u}{\partial t} + \frac{\partial u}{\partial a} = D(a)\frac{\partial^2 u}{\partial x^2} - d(a)u, \tag{1}$$

where $D(a)$ and $d(a)$ are the diffusion and death rates, respectively. Let τ be the total time spent from birth until becoming a sexually

* Corresponding author. Tel.: +1 (816) 235-2845.
E-mail address: baniyaghoubm@umkc.edu (M. Bani-Yaghoub).

http://dx.doi.org/10.1016/j.ecocom.2014.10.007
1476-945X/

mature adult. Then the total mature population at time t and position x is given by

$$w(x,t) = \int_{\tau}^{\infty} u(x,a,t)da. \tag{2}$$

By taking the integral from both sides of (1) and assuming that $u(t,\infty,x) = 0$, $D(a) = D_m$ and $d(a) = d_m$, we get

$$\frac{\partial w(x,t)}{\partial t} = u(x,\tau,t) + D_m \frac{\partial^2 w(x,t)}{\partial x^2} - d_m w(x,t), \tag{3}$$

where parameters D_m and d_m are diffusion and death rates of mature population, respectively. Using the method of separation of variables and Eq. (1), $u(x,\tau,t)$ can be replaced with an integral term. Then the nonlocal delay reaction-diffusion (RD) model of mature population is given by

$$\frac{\partial w(x,t)}{\partial t} = D_m \frac{\partial^2 w(x,t)}{\partial x^2} - d_m w(x,t) + \epsilon \int_{-\infty}^{\infty} b(w(y,t-\tau))\, f_\alpha(x - y)dy, \tag{4}$$

where $x \in \mathbb{R}$ and $0 < \epsilon \leq 1$. The first term on the right hand side of (4) reflects the spread of adults in the spatial domain and the second term corresponds to the mortality of adults. The function $b(w)$ is known as the birth function and $f_\alpha(x) = (1/\sqrt{4\pi\alpha})e^{-x^2/4\alpha}$ is the standard heat kernel which relates to random movement of individuals. Here $\alpha = \tau D_I > 0$, where D_I is the diffusion rate of immature population.

The integral term is a weighted spatial average that takes into account the local increase in the mature population due to migration of all individuals born elsewhere Gourley et al. (2004). In particular, the current mature population $w(x,t)$ at location x is increased by the weighted birth rates $b(w(y,t-\tau))$ at the previous time $t-\tau$ and all locations $y \in \mathbb{R}$. The term ϵ represents the survivorship of immature individuals from the time of birth until they are mature. This is given by

$$\epsilon = \exp\{-\int_0^{\tau} d_I(\theta)d\theta\}, \tag{5}$$

where $d_I(\theta)$ is the death rate of the immature population at age θ. Specifically, taking ϵ inside the integral term in (4) and considering $\epsilon b(w)$ as a single term, we may realize that the portion $(1-\epsilon)b(w)$ of individuals did not survive and therefore removed from the equation. This is similar to models that consider the mating probability $p(w)$ as a limiting factor of reproduction and include $p(w)b(w)$ rather than $b(w)$ Dennis (1989), McCarthy (1997), Wells et al. (1998).

Considering specific birth functions, the traveling wave solutions of model (4) have been previously studied Bani-Yaghoub and Amundsen (2014), Liang and Wu (2003), Liang et al. (2005). Moreover, model (4) has been further extended to RD models with two-dimensional spatial domains Liang et al. (2005), Weng et al. (2008), where the existence of traveling wave solutions Liang et al. (2005) has been investigated. Nevertheless the possible outcomes of model (4) in regards to extinction, survival or extinction-survival of a population remain poorly elaborated. The present work studies these outcomes by considering the general birth function $b(w)$, the maturation time τ and the diffusion rate D_m and D_I.

Similar to discrete models Anazawa (2009), the behavior of $b(w)$ can be classified into four categories: Indefinite Population Growth (IPG), Compensating Density Dependence (CD), Overcompensating Density Dependence (OCD) and Allee effect (AE), which are shown in Fig. 1. The OCD and the CD are two self-limiting mechanisms that arise from scramble competition and contest competition, respectively Nicholson (1954). The former represents a single species whose birth rate declines after it reaches a maximum value. Whereas the latter corresponds to a population with monotonic increase in the birth rate until it reaches some asymptotic value. The IPG occurs when $b(w)$ is increasing for all $w \geq 0$. Moreover, $b(w)$ may exhibit an AE Allee (1927, 1933) which often occurs at low population densities. The main concept of AE is

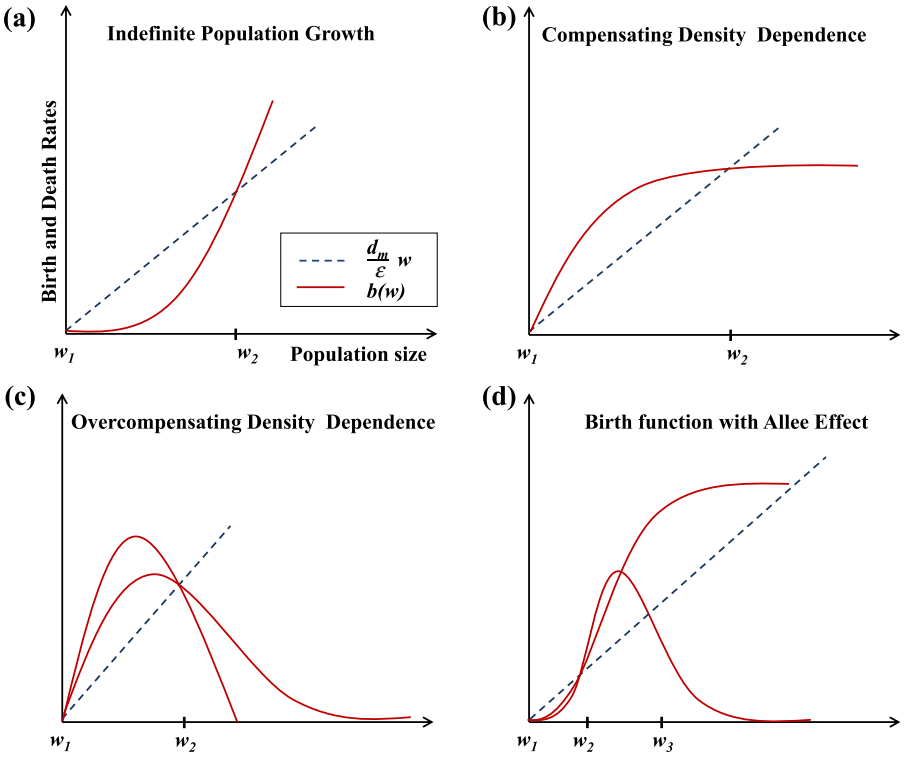

Fig. 1. A schematic representation of the density dependent birth function $b(w)$. Possible behaviors of $b(w)$ are indicated in each panel. The slope (d_m/ϵ) of the dashed lines indicates the ratio of the mature population death rate over immature population survival rate. The constant equilibria of model (4) are shown with w_1, w_2 and w_3.

that the density dependent per capita growth rate increases until the population reaches an optimal density, thereafter it reduces due to the increased population density. Mathematically, this corresponds to a birth function $b(w)$ with consecutive inflection point and maximum point.

Without considering the diffusion and the maturation time delay (i.e., $D_m = 0$, $D_I = 0$ and $\tau = 0$), model (4) is rewritten

$$\frac{dw(t)}{dt} = \epsilon w(t) g(w(t)), \tag{6}$$

where $g(w(t)) = (b(w(t))/w(t)) - (d_m/\epsilon)$ is the density dependent per capita net growth rate and (d_m/ϵ) is the ratio of the mature population death rate over immature population survival rate. Similar to Boukal and Berec (2002), the possible outcomes of the spatially homogeneous model (6) are classified as follows.

i. Extinction (**E**): The population goes extinct regardless of its initial size $w(0) = w_0$, when $g(w) < 0$ for all $w > 0$.
ii. Extinction-Survival (**ES**): Extinction or survival of the population depends on w_0. This is when $g(w) > 0$ in the interval between two positive equilibria and it is negative outside this interval.
iii. Survival (**S**): The population establishes at a positive equilibrium w_j, when $g(0) > 0$ and $g(w) < 0$ for all $w > w_j$.

Dispersal of mature and immature populations are considered in model (4) by the diffusion coefficients D_m and D_I, respectively. Whereas the reproduction and maturation are taken into account by birth function $b(w)$ and the delay term τ. Using model (4) the main objective of the present study is to develop a conceptual framework that expands outcomes (i)–(iii) according to the changes in dispersal, reproduction and maturation. In particular, how would the behavior of the birth function $b(w)$, the maturation time delay τ and the diffusion rates D_m and D_I affect the fate of the single species? The present study examines the local and global dynamics of the model (4) and employs various numerical simulations to unpack the interrelationships between $b(w), \tau, D_m$ and D_I. It will be shown that there is an interplay between maturation and reproduction that can determine the fate of the single species. Although population dispersal plays a role in the quality of the spatio-temporal patterns, it can neither change a model outcome to another, nor neutralize the impacts of maturation and reproduction. The interplay between the maturation and reproduction will be investigated according to the outcomes of model (4). Particularly, for species with an OCD birth function, the observed fluctuations of the spatial population densities can be as a result of the prolonged maturation time. This is not possible for species with a CD birth function. When the Allee effect and OCD are both taken into account, the prolonged maturation time can also be responsible for extinction of a single species. With a general birth function $b(w)$, it will be shown that the fate of a single species population can be determined at the beginning of the colonization by the ratio $\epsilon b'(0)/d_m$, maturation time delay τ and the initial population density in the spatial domain. Moreover, presence of a single species only in certain regions of the spatial domain can be explained by the stationary wave solutions of model (4).

Concerning the diffusion of the immature population, we may note that $D_I = \alpha/\tau$. Hence, the immature population is immobile when $\alpha = 0$ and the general model (4) is reduced to

$$\frac{\partial w(x,t)}{\partial t} = D_m \frac{\partial^2 w}{\partial x^2} - d_m w(x,t) + \epsilon b(w(x, t-\tau)), \tag{7}$$

which has been extensively studied Memory (1989), So and Yang (1998), So et al. (2000). A non-constant stationary wave solution $w(x,t) = \phi(x)$ of the reduced model (7) must satisfy

$$D_m \phi''(x) - d_m \phi(x) + \epsilon b(\phi(x)) = 0. \tag{8}$$

Let ϕ_1, ϕ_2 and ϕ_3 be three consecutive equilibria of (8). A solution of (8) that satisfies the boundary conditions $\phi(\pm\infty) = \phi_1$ is called a stationary pulse solution of the reduced model (7). Similarly, a stationary front solution of (7) satisfies the equation (8) and the boundary conditions $\phi(-\infty) = \phi_1$ and $\phi(+\infty) = \phi_3$. The stationary front and pulse solutions of (7) are respectively characterized by the homoclinic and heteroclinic orbits Guckenheimer and Holmes (1983), Jordan and Smith (1999) of Eq. (8) in their corresponding phase-planes. It will be numerically shown that these orbits can influence the solutions of the general model (4).

The rest of this paper is organized as follows. In Section 2 we study the impacts of dispersal, reproduction and maturation on the solutions of the reduced and the general model. In Section 3 the specific birth functions are introduced and the possible outcomes of model (4) are studied. In Section 4 the numerical simulations of the general and the reduced models are presented. In Section 5 a discussion of the main results is provided.

2. Impacts of dispersal, reproduction and maturation

The main objective of this section is to investigate the impacts of dispersal D_m and D_I, reproduction $b(w)$ and maturation time delay τ on dynamics of single species population. Depending on the behavior of the birth function $b(w)$, it is shown that the solution $w(x,t)$ of model (4) become oscillatory due to increased maturation time τ; both D_m and D_I can qualitatively change the spatio-temporal patterns of model (4); and D_m affects the stationary spatial patterns of the reduced model (7).

2.1. Stationary solutions influenced by dispersal

The energy function method Jordan and Smith (1999) can be applied to investigate the impacts of dispersal on the stationary solutions of the reduced model (7). Since the immature population is considered immobile (i.e., $D_I = 0$), we are only concerned with the impacts of D_m. Eq. (8) is written

$$\begin{cases} \dfrac{d\phi}{dx} = & \varphi \\ \dfrac{d\varphi}{dx} = & \dfrac{1}{D_m}(d_m\phi - \epsilon b(\phi)). \end{cases} \tag{9}$$

It can be verified that system (9) is a Hamiltonian system with the Hamiltonian function

$$H(\phi, \varphi) = \frac{\varphi^2}{2} + V(\phi), \tag{10}$$

where

$$V(\phi) = -\frac{1}{D_m}\int (d_m\phi - \epsilon b(\phi))d\phi \tag{11}$$

is the potential energy function. Using (10) the solution curves of the system (9) must satisfy

$$\varphi(\phi) = \pm\sqrt{2(s - V(\phi))}, \tag{12}$$

where s is an arbitrary constant. Suppose that the solution (12) consists of a homoclinic or a heteroclinic orbit $\Gamma(\phi)$, and the solution of model (4) or model (7) remains a neighborhood of $\Gamma(\phi)$ for a long period of time. Then the survival or extinction of the single species is determined by the stationary pulse or front solution $\phi(x)$ corresponding to $\Gamma(\phi)$. In Section 3 we will use specific birth functions to derive the exact homoclinic and heteroclinic orbits corresponding to the spatially dependent **ES** outcome. Moreover, Eq. (8) may admit periodic solutions, which represent a spatially dependent **S** outcome. If the solution of the reduced model (7) is attracted by a stationary periodic solution, then the population density varies periodically in the spatial

domain without going extinct. The following theorem provides orbital and sinusoidal approximations of such periodic solutions.

Theorem 1. *Let ϕ_j be a positive equilibrium of (8), then the orbits of (9) near $(\phi_j, 0)$ are approximated by*

$$2H(\phi_j, 0) + \varphi^2 + \gamma(\phi - \phi_j)^2 = k, \tag{13}$$

where $k \in (-\infty, \infty)$ is any constant and $\gamma = (\epsilon b'(\phi_j) - d_m)/D_m$. Furthermore if $\gamma > 0$, then orbits near $(\phi_j, 0)$ are closed and the periodic solutions are given by

$$\phi(x) = \frac{c}{\gamma}\sin(\sqrt{\gamma}x) + \phi_j, \tag{14}$$

where c is a positive constant.

The proof is given in Appendix B. Note that the existence of closed orbits and the periodic stationary solution $\phi(x)$ is possible when $\gamma > 0$ or equivalently $d_m/\epsilon < b'(\phi_j)$ for $\phi_j > 0$. To satisfy this condition we need to have $b'(\phi) > d_m/\epsilon$ for some $\phi > 0$. Otherwise, the following theorem indicates that the periodic solution $\phi(x)$ does not exist.

Theorem 2. *Let $b'(\phi) < d_m/\epsilon$ for all $\phi \in [0, \infty)$, then the system (9) has no closed orbit in $[0, \infty) \times \mathbb{R}$ and therefore the Eq. (8) has no periodic solution.*

The proof is based on Dulac's criterion (see Appendix B). The Eq. (8) and system (9) are independent of D_I and τ. Therefore, dispersal of immature population and maturation time delay have no impact of the stationary spatial patters of the reduced model (7). Theorem 1 and Eq. (14) indicate that the stationary solution $\phi(x)$ is influenced by the dispersal of mature population. Specifically, the amplitude and the frequency of $\phi(x)$ are proportional to D_m and $1/\sqrt{D_m}$, respectively.

Although $\phi(x)$ is the stationary solution of the reduced model (7), in Section 4 it will be numerically shown that the solutions of general model (4) can be initially attracted by the stationary pulse or front solutions of the reduced model (7). This is part of the bigger picture, where several dynamics of the reduced model are passed to the general model. In particular the next subsection addresses the stability of the equilibria, where the stability results are valid for both reduced and general models.

2.2. Delay-induced bifurcation

The linear stability analysis is applied to investigate the impacts of maturation time delay on the local dynamics of the general model (4). Let the solution $w(x,t)$ of model (4) in a neighborhood of the equilibrium w_j be in the form of $w(x,t) = w_j + \tilde{w}(x,t)$. Then substituting this form into (4), using the Taylor expansion of $b(w)$ about w_j, dropping nonlinear terms, and noting that $\epsilon b(w_j) - d_m w_j = 0$, the model linearized about w_j is given by

$$\frac{\partial \tilde{w}(x,t)}{\partial t} = D_m \frac{\partial^2 \tilde{w}(x,t)}{\partial x^2} - d_m \tilde{w}(x,t) + \epsilon b'(w_j) \int_{-\infty}^{\infty} \tilde{w}(y, t - \tau) f_\alpha(x-y) dy. \tag{15}$$

By letting $\tilde{w}(t,x) = e^{\lambda t + ikx}$, the last integral is calculated and the linearized model (15) is rewritten

$$\frac{\partial \tilde{w}(x,t)}{\partial t} = D_m \frac{\partial^2 \tilde{w}(x,t)}{\partial x^2} - d_m \tilde{w}(x,t) + \epsilon b'(w_j) e^{-\alpha k^2} \tilde{w}(x, t-\tau). \tag{16}$$

Moreover, the corresponding characteristic equation is given by

$$\lambda + D_m k^2 - \epsilon b'(w_j) e^{-(\alpha k^2 + \tau\lambda)} + d_m = 0, \tag{17}$$

where $k \in \mathbb{R}$ is the wave number.

Assuming the initial history function $w(x,t) = g(x)$ for $-\tau \le t \le 0$, the general solution of the linearized model (16) is given by

$$w(x,t) = \int_{-\infty}^{\infty} A(k) e^{\lambda(k,\tau)t + ikx} dk, \tag{18}$$

where the $A(k)$ is determined by a Fourier transform of $g(x)$. Here, we are concerned with the asymptotic solutions of Eq. (16) and there is no need to determine $A(k)$. If all eigenvalues have negative real parts, then w_j is a locally asymptotically stable equilibrium of the models (4) and (7).

The notation $\lambda(k,\tau)$ indicates that λ is a function of both k and τ. However, using the characteristic Eq. (17) it can be shown that for $Re(\lambda) < 0$ and $k = 0$, the magnitude of $Re(\lambda)$ will increase as the wave number k changes from zero. Hence the diffusion of the mature population can only increase the rate of convergence to w_j, but it will not result in loss of stability. The next Theorem classifies the local stability of w_j according to the behavior of the birth function $b(w)$.

Theorem 3. *Let w_j be a constant equilibrium of the model (4).*

(i) *if $|b'(w_j)| < d_m/\epsilon$, then w_j is locally asymptotically stable,*
(ii) *if $b'(w_j) - d_m/\epsilon > 0$, then w_j is unstable,*
(iii) *if $b'(w_j) + d_m/\epsilon < 0$, then w_j loses its stability when τ exceeds $\hat{\tau}$, where*

$$\hat{\tau} = (\pi - \arccos(-d_m/\epsilon b'(w_j)))/\sqrt{\epsilon^2 b'^2(w_j) - d_m^2} \tag{19}$$

is a Hopf bifurcation point.

The proof is given in Appendix A. Part *(i)* of Theorem 3 shows that the stability is delay independent if the slope of the birth function at w_j has a magnitude less than the ratio d_m/ϵ. This occurs for a positive equilibrium when a CD birth function is considered. Part *(ii)* is possible when an OCD birth function with AE is considered. Hence, a threshold value is defined for the **ES** outcome as follows. If $0, w_2$ and w_3 are three consecutive equilibria, where w_2 is the only unstable equilibrium. Then w_2 will be a threshold value and **S** is the outcome of the general model with an initial history function $w(x,t) > w_2$ for $t \in [-\tau, 0]$ and $x \in \mathbb{R}$. The outcome is **E** when the last inequality is reversed. Part *(iii)* is an extension to the Theorem 2.5.1 of Györi and Ladas (1991) and the stability result provided in Faria et al. (2006). Eq. (19) defines a different threshold based on the maturation time delay τ. In Section 4 we will numerically show that the spatio-temporal patterns near w_j will undergo several fluctuations when an OCD birth function is considered and the value of τ exceeds $\hat{\tau}$. Furthermore, the survival region in the spatial domain may shrink due to increased values of τ and an OCD birth function with AE.

Theorem 4. *If $b'(0) < d_m/\epsilon$ then the trivial solution of model (4) is locally asymptotically stable. Moreover, if in addition D_m, $D_I = 0$ and $0 < b(w(t)) \le b'(0)w(t)$ for all $t > -\tau$, then all positive solutions of (4) have asymptotic behavior $\lim_{t\to\infty} w(t) = 0$.*

Hence, regardless of any initial population density, a single species population will locally go extinct when $b'(0) < d_m/\epsilon$. The second part of Theorem 4 implies the global extinction however in the absence of diffusion (see Appendix B for the proof).

3. Possible outcomes of the general model

Using specific birth functions, we will investigate the possible outcomes of the general model (4). In addition to the classical outcomes, it will be shown that model (4) can provide space, time and delay dependent forms **E, S** and **ES**. Therefore, the complex

Table 1
List of the density dependent birth functions. The behavior of these birth functions are classified into four categories: overcompensating density dependence (OCD), compensating density dependence (CD), Allee Effect (AE) and indefinite population growth (IPG). See Fig. 1 for the schematic graph of these functions.

Birth function	Behavior (Fig. 1)	Case study	Refs.
$b_1(w) = pwe^{-aw^q}$	OCD (c^*)	Blowfly density oscillations	Gurney et al. (1980), Nicholson (1957)
$b_2(w) = pw/(1+aw^q)$	if $q<1$, IPG (a)	–	
	if $q=1$, CD (b)	Exploited fish populations	Beverton and Holt (1957)
	if $q>1$, OCD (c^*)	Traveling wavefronts	Liang and Wu (2003), Liang et al. (2005)
$b_3(w) = \begin{cases} pw(1-w^q/k_c^q) \\ 0 \text{ if } w>k_c \end{cases}$	OCD (c)	Whaling/fisheries management	Liang and Wu (2003), May (1980)
$b_4(w) = pw^2e^{-aw}$	OCD, AE (d^*)	Nonlinear population dynamics	Asmussen (1979), So et al. (2001)
$b_5(w) = pw^2/(1+aw)$	IPG (a)	–	Eskola and Parvinen (2007)
$b_6(w) = pw^2/(1+aw)^2$	CD, AE (d)	Models with Allee effect	Eskola and Parvinen (2007)

Notes. [1] *Parameters* p, q, k_c *and* a *and are all positive constants.* [2] *The notation* * *indicates the curves in Fig. 1 with right tail;* [3] *Birth functions* $b_5(w)$ *and* $b_6(w)$ *are special cases of the birth function used in the model proposed by Eskola and Parvinen (2007).*

dynamics of single species can be investigated with respect to the changes in dispersal, reproduction and maturation.

3.1. Spatio-temporal patterns and wave solutions

Table 1 represents the specific birth functions employed in this study. See also the corresponding schematic graphs shown in Fig. 1. As described below, these birth functions have been frequently used in various studies of single species. The birth function $b_1(w)$ was initially proposed by Nicholson Nicholson (1954, 1957) to study the oscillatory fluctuations in population density of sheep blowfly *Lucilia cuprina*. Later Gurney, Blythe and Nisbet Gurney et al. (1980) used $b_1(w)$ and extended the basic model (6) by including a discrete delay term. They showed a "humped" relationship between future adult recruitment and current adult population of blowflies. Moreover, $b_1(w)$ has been used in the reduced model (7) to investigate the asymptotic solutions Memory (1989), the numerical Hopf bifurcation So et al. (2000), solutions of the Dirichlet problem So and Yang (1998) and the traveling wave solutions Li et al. (2007), So and Zou (2001).

The birth function $b_2(w)$ with $q=1$ was first proposed by Beverton & Holt Beverton and Holt (1957) to study the dynamics of exploited fish populations. It can be shown that the birth function $b_3(w)$ is basically the same as the birth function proposed by May May (1980) which was used in studies of fisheries and whaling management. The work of Liang and Wu Liang and Wu (2003) considers the birth functions, $b_1(w)-b_3(w)$ to examine the traveling wave solutions and numerical approximations of model (4) with an extra advection term. The birth function $b_4(w)$ was first introduced by Asmussen Asmussen (1979) to study density dependent selection associated with Allee effect. Later Aviles Aviles (1999) used $b_4(w)$ to study the relation of nonlinearity and cooperation to evolution of sociality. The birth functions $b_5(w)$ and $b_6(w)$ are special cases of the birth function used in the model proposed by Eskola and Parvinen Eskola and Parvinen (2007).

The non-constant stationary solutions of the reduced model (7) include the homoclinic and heteroclinic orbits of the system (9). Specifically, a homoclinic orbit of system (9) represents a stationary pulse solution of the reduced model (7), whereas a heteroclinic orbit represents a stationary front. The following two theorems establish the conditions for existence of the homoclinic and heteroclinic orbits of the system (9).

Theorem 5. *The system (9) admits a homoclinic orbit if either of the conditions (i)–(iii) is satisfied.*

(i) $ae < \epsilon p/d_m$ *and* $b(\phi) = b_4(\phi)$.
(ii) $a < \epsilon p/d_m$ *and* $b(\phi) = b_5(\phi)$.
(iii) $4a < \epsilon p/d_m$ *and* $b(\phi) = b_6(\phi)$.

Theorem 6. *Let* $\epsilon p/d_m = e^r a/r$, *where* $r \approx 1.451$ *is the root of* $-2e^k/k + k^2/2 + k + 2 + 2/k$. *Then system (9) with birth function* $b_4(\phi)$ *has a heteroclinic orbit. Moreover, there exists no heteroclinic orbit when* $b_6(\phi)$ *is considered.*

See Appendix B for the proofs of Theorems 5 and 6.

The general model (4) has the same constant equilibria as the reduced model (7), and the system (9). The expressions for these equilibria are indicated in the second column of Table 2. The third column of Table 2 provides the conditions for existence of the constant equilibria. Moreover, the conditions inside the parentheses are for existence of the stationary pulses and the stationary front of the reduced model (7) characterized by the homoclinic and

Table 2
The nontrivial equilibria of the models (4) and (7). The existence conditions for the stationary pulse and front are indicated in the parentheses. The last three columns indicate the stability of constant equilibria. Those shown inside parentheses relate to the system (9)

Function	Positive equilibria	Existence conditions	w_1	w_2	w_3
$b_1(w)$	$w_2 = (\ln(\epsilon p/d_m)/a)^{1/q}$	$\epsilon p/d_m > 1$	U	AS	–
$b_2(w)$	$w_2 = ((\epsilon p - d_m)/ad_m)^{1/q}$	$\epsilon p/d_m > 1$	U	AS	–
$b_3(w)$	$w_2 = k_c(1 - d_m/\epsilon p)^{1/q}$	$\epsilon p/d_m > 1$	U	AS	–
$b_4(w)$	$w_2 = -W_0(-ad_m/\epsilon p)/a$	$\epsilon p/d_m > ae$	AS (S)	U (C)	AS (S)
	$w_3 = -W_{-1}(-ad_m/\epsilon p)/a$	($cond^1$ or $cond^2$)			
$b_5(w)$	$w_2 = d_m/(\epsilon p - ad_m)$	$\epsilon p/d_m > a$ ($cond^3$)	AS (S)	U (C)	–
$b_6(w)$	$w_2, w_3 = (\epsilon p - 2ad_m \pm \sqrt{\epsilon p(\epsilon p - 4ad_m)})/2a^2d_m$	$\epsilon p/d_m > 4a$ ($cond^4$)	AS (S)	U (C)	AS (S)

Notes: $W_0(x)$ *and* $W_{-1}(x)$ *represent the real-valued principal and the lower branches of Lambert* $W(x)$ *function, for* $x \in (-e^{-1}, 0)$. *For models (4) and (7) the equilibria are classified as AS: locally asymptotically stable and U: unstable. By Theorem 3 stability of* w_j *can be delay dependent. The equilibria of system (9) are classified as (S): saddle and (C): center. For the existence of the stationary pulse,* $cond^1$: $\epsilon p/d_m > ae$, $cond^3$: $\epsilon p/d_m > a$ *and* $cond^4$: $\epsilon p/d_m > 4a$ *(Theorem 5). For the existence of the stationary front,* $cond^2$: $\frac{\epsilon p}{d_m} \approx 2.94a$ *(Theorem 6).*

the heteroclinic orbits of the system (9). The last three columns of Table 2 represent the stability of the positive constant equilibria. The stability results are the same for the reduced and the general model, but different when system (9) is considered. As indicated inside the parentheses, the equilibria of system (9) are classified as saddle or center. For the reduced and general model the stability of the equilibria can be delay dependent if $b'(w_j) + d_m/\epsilon < 0$ (see Theorem 3). This is possible when $\epsilon p/d_m$ is large and $b_1(w) - b_4(w)$ are considered. In Section 4 it will be shown that the bifurcating the solutions of model (4) result in the spatio-temporal patterns of single species densities.

3.2. Classical versus new outcomes

The specific outcomes of the general model (4) and the required conditions are summarized in Table 3. In addition to the classical outcomes **E, S** and **ES**, the general model (4) is capable of generating delay and space dependent **S** and **ES**. The space and delay dependent survival is denoted by **S(x, τ)**, which is only possible when a birth function without AE is considered. Specifically, when $b(w) = b_i(w), i = 1, 2, 3$ and the conditions stated in the fourth column are satisfied, survival of the single species in the spatial domain is delay dependent. If the maturation time delay τ is greater than the threshold $\hat{\tau}$ defined in Eq. (19), then stability of w_2 is lost and eventually oscillatory solutions $w(x, t)$ will bifurcate from w_2. The space and delay dependent extinction-survival outcome is denoted by **ES(x, τ)**, which is only possible when an OCD birth function with AE is considered. Namely, with $b_4(w)$ and $\epsilon p/d_m > 3/a$, the location of the single species and the magnitude of the maturation time delay determine the extinction or survival of the population. When the delay τ is substantially increased the population goes extinct in the entire spatial domain (see **ES(x, τ)** → **E** in Table 3). Delay has no effect if a CD birth function with AE, such as $b_6(w)$ is considered. With an IPG birth function such as $b_5(w)$, the equilibrium w_2 is unstable and it is not bounded by any other equilibrium. Then for single species with initial population densities greater than w_2 in the spatial domain, the general model (4) results in unbounded population densities, which is not realistic. The spatio-temporal extinction-survival outcomes are denoted by **ES^1(x, t)** and **ES^2(x, t)**. These outcomes are respectively possible when the solutions of model (4) remain in a neighborhood of a stationary pulse and a stationary front of model (7) for a long period of time. The numerical simulations confirm the last two outcomes when an OCD birth function with AE is considered.

4. Numerical simulations

Using a finite difference method and Matlab 2014a, the general model (4) and the reduced model (7) were explored for different sets of parameter values, initial conditions and the specific birth functions. We also used Matlab ODE 45 and the toolbox "pplane8" to numerically verify the existence of periodic stationary solutions, stationary pulses and fronts of the reduced model (7).

4.1. Formation of stationary pulse and front

Fig. 2(a) and (c) represent the phase-planes of the system (9) when birth function $b_4(w)$ was considered (see Theorem 5 part (i) and Theorem 6). The corresponding stationary pulse and front solutions of the reduced model (7) are shown with the dashed lines in panels (b) and (d), respectively. Moreover, the periodic solutions (shown with solid lines) relate to the closed orbits in the phase-planes. The periodic solutions represent periodic forms of survival in the spatial domain, whereas the stationary pulse in panel (b) and the stationary front in panel (d) represent spatially dependent **ES** outcomes. Note that we did not impose any phase condition Doedel and Friedman (1989), Friedman and Doedel (1991) and therefore the stationary solutions may occur anywhere in the spatial domain. Specifically, for any constant c, both $\phi(x)$ and $\phi(x + c)$ are the solutions of the Eq. (8) satisfying the boundary conditions $\phi(\pm\infty) = 0$. Imposing a phase condition can be unrealistic because it requires a template function that is practically unknown. Similarly, the dashed line in panel (d) represents a stationary front that may occur anywhere in the spatial domain. The specific parameter values used to generate Fig. 2 are $\epsilon = 0.1, D_m = 3, p = 0.1, a = 0.4, d_m = 0.0075$ for panels (a) and (b), and $d_m = 0.0085$ for panels (c) and (d).

The numerical simulations suggest that the solution of the general model (4) can be initially attracted by the stationary pulse or front solutions of the reduced model (7). However, the actual convergence to the stationary pulse or front doesn't seem to occur. As shown in panel (a) of Fig. 3, the solution of the general model (4) first approaches to the stationary pulse of model (7), then it slowly moves away and converges to the spatially homogenous equilibrium $w_3 = 4.45$ (see Table 2, row 4). Panel (b) of Fig. 2 represents the approach to the stationary pulse (see the animation file mmc4.gif available in the supplementary data). Also, the final convergence to w_3 is shown in the animation mmc7.gif. This behavior may resemble that of solutions around a saddle for a

Table 3
Possible outcomes of the general model (4) and the required conditions. Classical outcomes are the same as those of spatially homogeneous single species model (6). Whereas the new outcomes are only possible for the general model (4).

Function	Classical outcomes		New outcomes	
	S	**E**	**S → S(x, τ)**	
$b_1(w)$	$\epsilon p/d_m \in (1, e^{2/q})$	$\epsilon p/d_m < 1$	$\epsilon p/d_m > e^{2/q}$	
$b_2(w)$	$\epsilon p/d_m \in (1, q/(q-2))$	$\epsilon p/d_m < 1$	$\epsilon p/d_m > q/(q-2)$	
$b_3(w)$	$\epsilon p/d_m \in (1, (q+2)/q)$	$\epsilon p/d_m < 1$	$\epsilon p/d_m > (q+2)/q$	
	ES	**E**	**ES → ES(x, τ)**	**ES(x, τ) → E**
$b_4(w)$	$\epsilon p/d_m \in (ae, 3/a)$	$\epsilon p/d_m < ae$	$\epsilon p/d_m > 3/a$	$\epsilon p/d_m > 3/a$, τ large
$b_5(w)$	$\epsilon p/d_m > a$	$\epsilon p/d_m < a$		
$b_6(w)$	$\epsilon p/d_m > 4a$	$\epsilon p/d_m < 4a$		
			ES^1(x, t)	**ES^1(x, t) → S** or **E**
$b_4(w)$			$\epsilon p/d_m > ae$	$\epsilon p/d_m > ae$, t large
$b_6(w)$			$\epsilon p/d_m > 4a$	$\epsilon p/d_m > 4a$, t large
			ES^2(x, t)	
$b_4(w)$			$\epsilon p/d_m \approx 2.94a$	

Notes. The outcomes are classified into **S, E, ES***: space and delay independent Survival, Extinction, Extinction-Survival, respectively;* **S(x, τ)***: space and delay dependent survival;* **ES(x, τ)***: space and delay dependent Extinction-Survival;* **ES^1(x, t)***: space and time dependent Extinction- Survival with survival only in a narrow region of the spatial domain; and* **ES^2(x, t)***: space and time dependent Extinction-Survival with survival in the entire left or right half of the spatial domain. With the birth function $b_5(w)$ extinction occurs only when initial population density is less than w_2. Otherwise, the population density reaches infinity, which is not biologically realistic.*

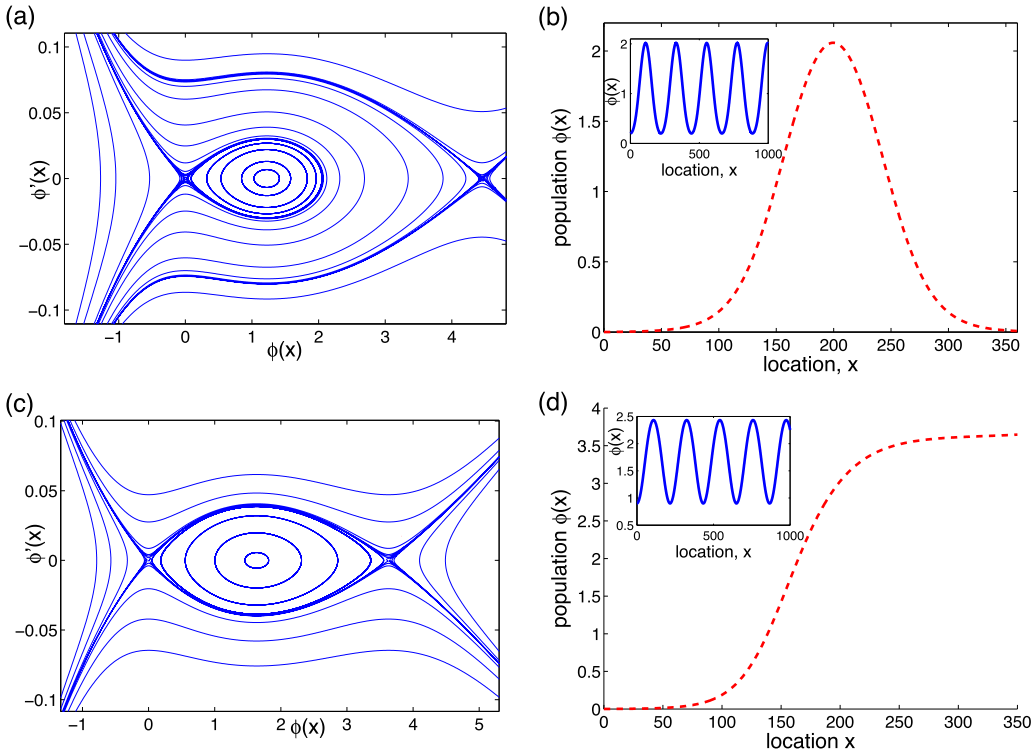

Fig. 2. The phase-plane and the stationary solutions of the reduced model (7). (a) The homoclinic orbit and the equilibrium solutions of Eq. (8); (b) the stationary pulse (shown with dashed line) corresponding to the homoclinic orbit. The inner panel represents a periodic solution of Eq. (8); (c) the heteroclinic orbit and the equilibrium solutions of Eq. (8); (d) the stationary front (shown with dashed line) corresponding to the heteroclinic orbit. We considered $b_4(w)$ and the parameter values $\epsilon = 0.1, D_m = 3, p = 0.1, a = 0.4$, $d_m = 0.0075$ for panels (a and b) and $d_m = 0.0085$ for panels (c and d).

system of ordinary differential equations. Particularly, the solution $w(x,t)$ of the initial value problem first approaches to the stationary pulse and then it moves away and follows the stable manifold of w_3. Note that the initial history function is a determining factor in the convergence of $w(x,t)$ to the trivial equilibrium or w_3. Here we considered $w(x,t) = w_2 - y_0 + 0.2\exp(-0.001(x - x_0)^2)$, with $t \in [-\tau, 0], w_2 = 1.22, y_0 = 0.04$ and $x_0 = 222$, where w_2 is the unstable equilibrium of the general model. The value of x_0 corresponds to the peak of the stationary wave in panel (b). Hence, instead of the phase condition Doedel and Friedman (1989), Friedman and Doedel (1991), the initial population densities in the spatial domain can be employed to determine the peak and the actual location of the stationary solution in the spatial domain. By changing the value of x_0, the solution $w(x,t)$ is initially attracted by the same stationary pulse that is shifted to the left or right. Furthermore, increasing the value of y_0 will result in convergence to the trivial equilibrium. This corresponds to $\mathbf{ES^1(x,\ t) \to E}$ in Table 3. Whereas decreasing the value of y_0 results in convergence to $w_3 = 4.45$, which represents $\mathbf{ES^1(x,\ t) \to S}$ in Table 3. This highlights the dependance of the model outcomes to the initial history function. Panels (c) and (d) of Fig. 3 illustrate that the solution $w(x,t)$ of the general model (4) remain in a neighborhood of the stationary front $\phi(x)$ of the reduced model (7) for a long period of time. This corresponds to $\mathbf{ES^2(x,\ t)}$ in Table 3. The initial history function is $w(x,t) = w_2 - y_0 + 0.2/(1 + \exp(-0.043(x - x_0)))$ for $t \in [-\tau, 0], y_0 = 0.1, w_2 = 1.63$ and $x_0 = 210$. Again, changing x_0 value will shift the stationary front and changing the y_0 value will result in convergence to the equilibrium $w_1 = 0$ or $w_3 = 3.63$. Animation mmc3.gif in the supplementary data shows that the solution of model (4) is attracted by the stationary front. For Fig. 3 we considered $\tau = 1$ and $D_I = 1$. All other parameter values are the same as those used for generating Fig. 2.

4.2. Delay-induced spatial patterns

Fig. 4 represents the destabilizing effects of delay τ for $b(w) = b_1(w), d_m = .05, \epsilon = 0.2, p = 5, a = 1, q = 1$ and the initial history function $w(t,x) = 1 + \cos(x/10)$, for $t \in [-\tau, 0]$. Namely, in the absence of diffusion (i.e., D_m, $D_I = 0$), panel (a) shows that the oscillatory and periodic solutions bifurcate from the positive equilibrium w_2 due to increases in τ (see the animation mmc5.gif). When the diffusion of mature and immature populations are included (i.e., when D_I, $D_m > 0$), the spatial patterns are substantially changed as τ is increased. As shown in panels (b)–(d) of Fig. 4, the changes in the spatial patterns can be traced back to the bifurcating solutions presented in panel (a). Hence the survival of a single species population (that is established at a positive stable equilibrium) changes to a survival with fluctuating values of the population density in the spatial domain (see $\mathbf{S \to S(x,\ \tau)}$ in Table 3). The transitions of spatial patterns from (b) to (d) are shown in movie clip mmc1.gif. Considering part *(iii)* of Theorem 3, similar results were obtained using different parameter values, initial history functions and birth functions $b_1(w) - b_3(w)$. Hence, delay dependence of the positive equilibrium can play a crucial role in the spatial patterns of the general and reduced models.

As mentioned before, the reduced model (7) represents dynamics of a single species whose immature population is immobile (i.e., $D_I = 0$). To numerically observe the impacts of immature population dispersal, we may compare the solutions $w_r(x,t)$ and $w_g(x,t)$ corresponding to the reduced model (7) and

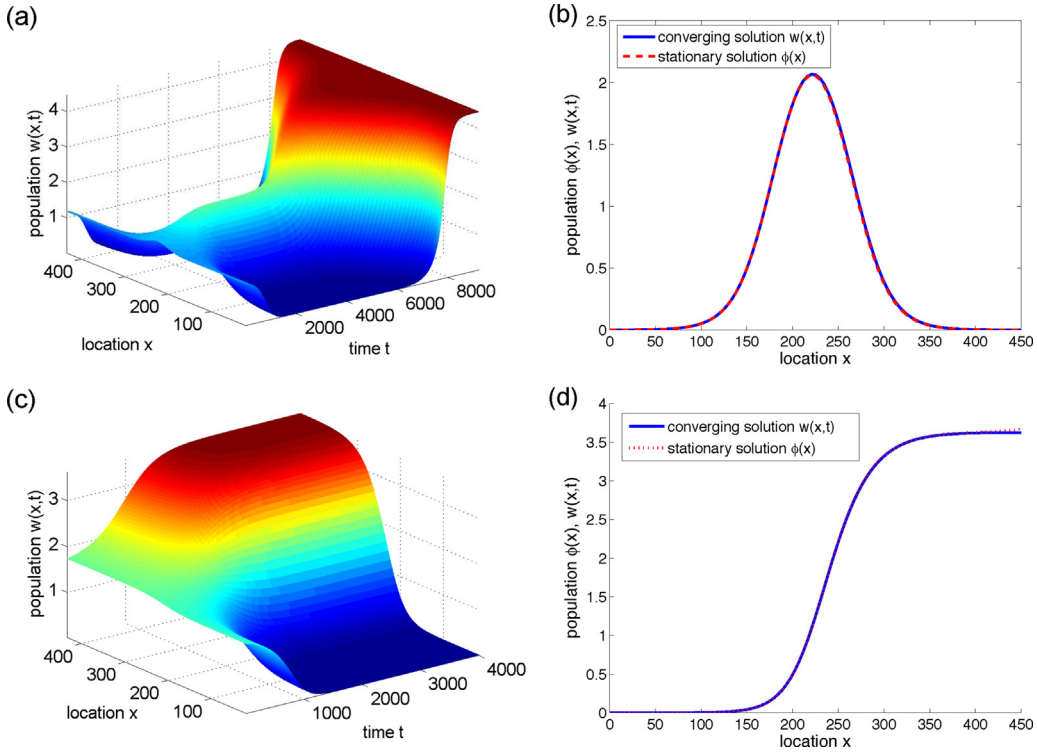

Fig. 3. The solutions of the general model (4) can approach to the stationary solutions of the reduced model (7). (a) The solution $w(x,t)$ initially approaches to the stationary pulse solution $\phi(x)$. Thereafter it converges to the constant equilibrium w_3. See the movie clip mmc7.gif available in the supplementary data. (b) Initial approach to the stationary pulse. See the movie clip mmc4.gif. (c and d) The solution $w(x,t)$ approaches to the stationary front solution $\phi(x)$. See the movie clip mmc3.gif.; Here, $\tau = 1$, $D_I = 1$ and the other parameter values are the same as those used to generate Fig. 2. The initial history functions related to panels (a) and (c) are $w(x,t) = w_2 - 0.04 + 0.2\exp(-0.001(x-222)^2)$ and $w(x,t) = w_2 - 0.1 + 0.2/(1+\exp(-0.043(x-210)))$, with $t \in [-\tau, 0]$, respectively.

the general model (4), respectively. Let $R(x,\ t)$ be the relative difference between the spatial patterns generated by $w_r(x,t)$ and $w_g(x,t)$ defined by

$$R(x,t) = \frac{|w_g(x,t) - w_r(x,t)|}{w_g(x,t)}. \tag{20}$$

Then $R(x,\ t)$ measures the influence of immature population dispersal on the spatio-temporal patterns. Namely, panels (e) and (f) of Fig. 4 represent the relative differences between the spatial patterns generated with the reduced and the general models. It can be seen that the magnitude of $R(x,\ t)$ drops as t increases. Nevertheless the relative differences further spread in the spatial domain, when τ is increased.

Although the spatio-temporal patterns are greatly influenced by the choice of the initial history function, we numerically observed that the impact of the initial function on the spatial patterns vanishes over the time. Whereas the oscillations due to large values of delay (e.g., $\tau = 50$) persist. This may suggest an approximate solution of the form $w(x,t) = \psi(x)u_\tau(t)$, where $u_\tau(t)$ is the solution of the model (4) with $D_I = 0$, $D_m = 0$ and $\psi(x)$ is a continuous function that converges to a positive constant as $t \to \infty$.

We also explored the impact of mature population dispersal on the spatio-temporal patterns. By increasing the value of D_m, we noticed that the influence of the initial condition on the spatial patterns disappears in a shorter period of time. However, regardless of D_m values, the oscillation due to the delay-induced bifurcating solutions persists.

4.3. Formation of traveling wavefront

Fig. 5(a) represents a numerical verification of Theorem 4 when the birth function $b_3(w)$ is used. Under the conditions of Theorem 4, the extinction of single species is independent of τ and the initial population density. The specific parameter values are $d_m = 0.33$, $\tau = 10$, $\epsilon = 0.1$, $p = 4$, $q = 1$ and $k_c = 5$ (and $D_m = 0.5$, $D_I = 0.1$ for the inner panel). Fig. 5 (b)-(d) illustrates the **ES(x, τ)** $\to$ **E** scenario in Table 3, where the survival region in the spatial domain is eventually vanished as τ increases. Here we considered $b(w) = b_4(w), w(0,x) = w_2 + 0.1\cos(x/10),\ p = 4, a = 1, \epsilon = 0.1, d_m = 0.05, D_m = 0.5$ and $D_I = 1/\tau$. By part *(iii)* of Theorem 3, when $\epsilon b'(w_3) + d_m < 0$, the stability of the equilibrium w_3 is lost when τ is increased. Using the above values we get that $w_1 = 0$ is stable and delay independent, $w_2 = 0.14$ is unstable and $w_3 = 3.2617$ is stable but delay dependent. By increasing τ the triangular region of survival (see panel (c) of Fig. 5) shrinks and ultimately disappears. This is due to the loss of the stability of w_3 and the change of the bistable to the monostable case. Therefore, the single species goes extinct when τ is increased. The movie clip mmc2.gif representing the transition from (b) to (d) is provided in the supplementary data. Despite the case $b(w) = b_1(w)$, here the initial history function and the maturation time delay may determine the fate of the single species population. It can be numerically shown that the single species will survive if $w(t,x) > w_2$ for all $x \in \mathbb{R}, t \in [-\tau, 0]$ and τ small, whereas it goes extinct when the last inequality is reversed. This coincides with the classical **ES** outcome (see the second column of Table 3). Moreover, Fig. 5 (c) represents the formation of the traveling wavefronts in the spatial domain. Previous studies have established the existence of the traveling wave solutions for the bistable case (see Gourley et al. (2004) and

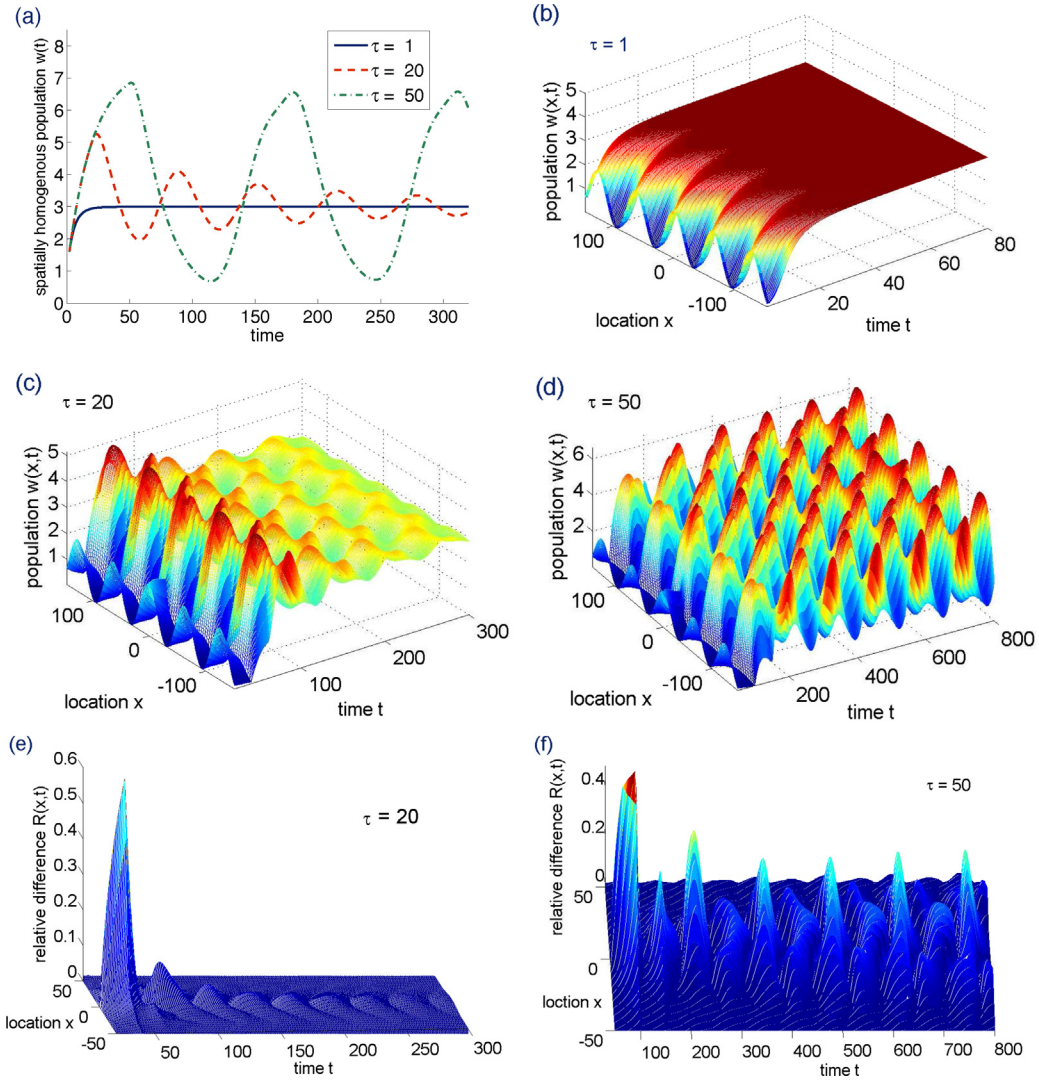

Fig. 4. Impacts of the maturation time delay on stability of w_2 and the spatial patterns of the single species. We considered $b(w) = b_1(w), d_m = .05, \epsilon = 0.2, p = 5, a = 1, q = 1$ and $w(t,x) = 1 + \cos(x/10)$, for $t \in [-\tau, 0]$ (a) In the absence of diffusion (i.e., when $D_m, D_l = 0$), the oscillatory and periodic solutions bifurcate from the equilibrium w_2 when τ is increased. See the movie clip mmc5.gif available in the supplementary data; (b–d) Inclusion of the diffusion (i.e., when $D_m = 0.5$, $D_l = 1/\tau$) generates spatio-temporal patterns that are sensitive to the value of τ. Animation mmc1.gif shows the transition from (b) to (d); (e) the relative difference between the spatial patterns generated by the reduced model (7) and the general model (4) for $\tau = 20$; (f) as τ increases, the differences spread more in the spatial domain.

the references therein). However the formation of the traveling wavefronts has been less examined. The file mmc6.gif is the animation of panel (c), which illustrates the formation of the traveling wavefronts of model (4) in the spatial domain. Note that a monotonic traveling wavefront of the general model may become oscillatory when the diffusion ratio D_l/D_m is greater than a critical value d_c and the slope of the birth function at the nontrivial equilibrium is negative (see proposition 2 and Section 4 of Bani-Yaghoub and Amundsen (2014)).

5. Discussion

The present work was an attempt to investigate the interrelationships between dispersal D_l, D_m, reproduction $b(w)$, and maturation τ according to the outcomes of the general model (4). We showed that the single species dynamics are greatly influenced by the interplay between maturation and reproduction as opposed to dispersal. Theorem 3 shows that the impact of the maturation time delay τ on the population dynamics is highly dependent on the slope of the birth function $b(w)$ at the positive equilibrium w_j. Particularly, with a CD birth function, the classical **S** outcome and the spatial patterns remain delay independent. However, as shown in Fig. 4(b)–(d), an OCD birth function may result in space and delay dependent **S**. With the AE and OCD, Fig. 5(b)–(d) shows that the increases in the delay may change the **ES** outcome defined by the traveling wavefronts in panel (c) to **E** outcome in panel (d).

The destabilizing impacts of delay have been previously shown for spatially homogeneous models Gopalsamy (1992), Gurney et al. (1980), Kuang (1993). The stability conditions of Theorem 3 are similar to those of the Theorem 2, page 70 of Kuang (1993) and Section 2.3 of Gopalsamy (1992). Here we showed that the impacts of maturation time delay and the birth function remain present for models that include delay, diffusion and nonlocality. The numerical simulations indicate that different values of the mature diffusion rate D_m result in qualitatively different spatial patterns. However, the changes in D_m can neither overcome the oscillations caused by the maturation time delay τ nor alter the **E, S** or **ES** outcome. Hence the impact of D_m on the spatial patterns is less dominant, as opposed to the impacts of τ and $b(w)$.

Depending on the initial population densities of the single species in the spatial domain, the spatially dependent **ES** outcome

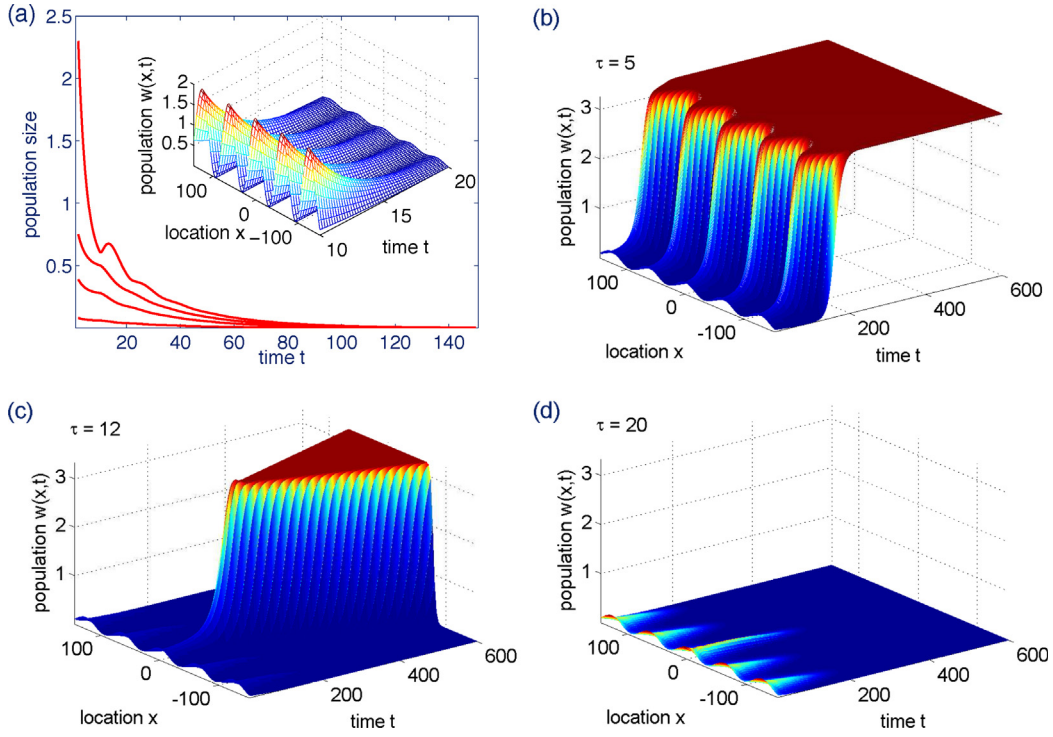

Fig. 5. Population extinction may occur due to the restriction on the birth function (see Theorem 4) or due to delay increases (see part (iii) of Theorem 3). (a) The population goes extinct irrespective of the initial population density and the values of τ (see Theorem 4). Here we considered $b(w) = b_3(w), k_c = 5, q = 1, p = 2, \epsilon = 0.1, d_m = 0.33, \tau = 10$ and ($D_m = 0.5, D_l = 0.1$ for the inner panel). (b)-(d) Simulation of the case **ES(x, τ)** → **E** for $b_4(w)$ in Table 3. We considered $b(w) = b_4(w), p = 4, a = 1, \epsilon = 0.1, d_m = 0.05, D_m = 0.5$ and $D_l = 1/\tau$. The initial history function is $w(t, x) = w_2 + 0.1\cos(x/10)$, where $t \in [-\tau, 0]$. The value of τ has been indicated in each panel. The movie clip mmc2.gif representing the transition from (b) to (d) is available in the supplementary data. Also mmc6.gif animates the formation of traveling wavefronts as shown in panel (c).

may gradually change to the classical **E** (Fig. 5 (c),(d)) or **S** outcome. Particularly, as shown in Fig. 3 (a), first the survival occurs only in a narrow region of the spatial domain and thereafter, the survival in the narrow region will extend to the survival in the entire spatial domain. By Theorem 6 a CD birth function with AE may give rise to a stationary wavefront, which represents a different quality of spatially dependent **ES**. Namely, the survival occurs in the entire left-half or right-half of the spatial domain. This is shown in panels (c) and (d) of Fig. 3, where the spatially inhomogeneous initial population densities above and below the unstable equilibrium w_2 lead to formation of the stationary wavefront.

Theorems 5 and 6 are limited to specific birth functions. However, they establish conditions for existence of stationary pulse and front solutions of the reduced model (7). The existence and formation of the stationary solutions may explain certain ecological mechanisms as follows. Formation of a stationary pulse in the spatial domain may correspond to the directional movement of individuals that are initially scattered in the spatial domain and they gradually form a breeding area (Yadav (2006), chapter 6).

Table 3 is a collection of the possible model outcomes when the specific birth functions are used. These birth functions cover a wide range of ecological concepts indicating the widespread applicability of the model analysis provided in this study. Note that the ratio $\epsilon p/d_m$ is originated from the ratio $\epsilon b'(0)/d_m$, where $b'(0)$ may represent the rate of colonization at low population densities. Hence, the fate of a single species population can be determined at the beginning of the colonization by the ratio $\epsilon b'(0)/d_m$ and the initial population densities in the spatial domain. For instance, as shown in the fourth column of Table 3, space and delay dependent survival is predicted if this ratio exceeds certain threshold values.

In conclusion, the present study lays the foundations for a deeper understanding of single species dynamics through analysis of a nonlocal delay RD model. The new and classical model outcomes may enable the researchers to trace back the main causes of the spatio-temporal density fluctuations according to the changes in dispersal, maturation and reproduction.

Acknowledgments

The authors would like to thank the anonymous reviewers for their valuable suggestions and their roles in strengthening the results of this paper. This work was partially supported by the University of Missouri-Kansas City startup fund MOcode: KCS21.

Appendix A. Details on local stability analysis

Proof of Theorem 3,

Part *(i)*

When $\tau = 0$ the characteristic Eq. (17) is reduced to $\lambda = \epsilon b'(w_j)e^{-\alpha k^2} - d_m - D_m k^2$. Since $|b'(w_j)| < d_m/\epsilon$, $\lambda < 0$ for all $k \in \mathbb{R}$ and $\alpha \geq 0$. Hence w_j is asymptotically stable. Let $\tau > 0$. Assume that the characteristic Eq. (17) has a root $\lambda = u + iv$ where $u \geq 0$ for some $\tau > 0$. Substituting $\lambda = u + iv$ into (17) and equating the real part and the imaginary part to zero we get that

$$D_m k^2 + u + d_m - \epsilon b'(w_j)e^{-(\alpha k^2 + u\tau)}\cos(\tau v) = 0, \tag{A.1}$$

$$v + \epsilon b'(w_j)e^{-(\alpha k^2 + u\tau)}\sin(\tau v) = 0. \tag{A.2}$$

Moving the terms with sine and cosine to the right-hand side, squaring them and adding them together, we obtain

$$(D_m k^2 + u + d_m)^2 + v^2 = \epsilon^2 b'^2(w_j)e^{-2(\alpha k^2 + u\tau)}. \tag{A.3}$$

Since $\tau, \alpha, u \geq 0$ we get that

$$(D_m k^2 + u + d_m)^2 + v^2 \leq \epsilon^2 b'^2(w_j). \tag{A.4}$$

Expanding the first term in (A.4) we have

$$2D_m k^2 d_m + 2D_m k^2 u + D_m^2 k^4 + u^2 + 2ud_m + v^2 \leq \epsilon^2 b'^2(w_j) - d_m^2. \tag{A.5}$$

Since $u \geq 0$, the left-hand side of (A.5) is positive whereas the right-hand side of (A.5) is negative due to $\epsilon|b'(w_j)| < d_m$. This is a contradiction.□

Part *(ii)*

When $\tau = 0$, using the characteristic Eq. (17) we get that w_j is unstable for some k. When $\tau > 0$, define

$$h_j(\lambda) = \lambda + d_m + D_m k^2 - \epsilon b'(w_j) e^{-(\alpha k^2 + \tau\lambda)}, \tag{A.6}$$

where $h_j(\lambda) = 0$ represents the characteristic Eq. (17). Since $\epsilon b_i'(w_j) - d_m > 0$, we have $h_j(0) < 0$ for some k. Moreover $h_j(\lambda)$ is a continuous function of λ and $\lim h_j(\lambda) = \infty$ as $\lambda \to \infty$. By the intermediate value theorem h_j has a real positive root and therefore w_j is unstable.

Part *(iii)*

Similar to Faria et al. (2006) we show that there is a pair of pure imaginary eigenvalues corresponding to w_j when $\tau = \hat{\tau}$. Let $\lambda = i\omega$, $\omega \in \mathbb{R}$ and $k = 0$. From (17) we get that

$$i\omega = -d_m + \epsilon b'(w_j)(\cos(\omega\tau) - i\sin(\omega\tau)), \tag{A.7}$$

where $\epsilon b'(w_j)$ is the derivative of $b(w)$ evaluated at w_j. Separating (A.7) into imaginary and real parts we have

$$\begin{cases} d_m &= \epsilon b'(w_j)\cos(\omega\tau), \\ \omega &= \epsilon b'(w_j)\sin(\omega\tau). \end{cases} \tag{A.8}$$

Squaring these two equations and adding them together result in,

$$\omega^2 = \epsilon b'^2(w_j) - d_m^2. \tag{A.9}$$

By choosing $\omega > 0$, we get that

$$\omega = \sqrt{\epsilon b'^2(w_j) - d_m^2}. \tag{A.10}$$

Substituting (A.10) into the first equation of (A.8) and solving for τ, the specified form of $\hat{\tau}$ is obtained. Clearly, if $\epsilon b'(w_j) + d_m < 0$, then for $\tau = \hat{\tau}$, the characteristic Eq. (17) has a pure imaginary root $\lambda = i\omega$ and therefore w_j cannot be asymptotically stable.

Our next step is to show that w_j loses its stability when τ exceeds $\hat{\tau}$. Considering λ as a function of τ, we are only required to show that the real part of derivation of λ at iw is positive (i.e., as τ is increased from $\hat{\tau}$, $\lambda = iw$ falls into the right half of the complex plane). Taking the derivative of the characteristic Eq. (17) and given that ϵ is a function of τ we have

$$\lambda' + \epsilon b'(w_j) e^{-\tau\lambda}(\lambda + \tau\lambda' - d_l(\tau)) = 0, \tag{A.11}$$

where λ' denotes the derivative of λ with respect to τ. From Eq. (17) we have $\epsilon b'(w_j) e^{-\tau\lambda} = \lambda + d_m$, then (A.11) is rewritten

$$\lambda' = \frac{(\lambda + d_m)(d_l(\tau) - \lambda)}{(1 + \tau(\lambda + d_m))}. \tag{A.12}$$

By evaluating λ' at iw we have

$$\lambda'(iw) = \frac{(iw + d_m)(d_l(\tau) - iw)}{(1 + \tau(iw + d_m))}. \tag{A.13}$$

Multiplying the numerator and denominator of (A.13) by $1 + \tau d_m - i\tau w$, the real part of $\lambda'(iw)$ is given by

$$Re\lambda'(iw) = \frac{(d_l(\tau)(\tau(d_m^2 + w^2) + d_m) + w^2)}{((1 + \tau d_m)^2 + (\tau w)^2)}. \tag{A.14}$$

Since $Re\lambda'(iw) > 0$, it implies that there is an eigenvalue with positive real part as τ increases from $\hat{\tau}$. This completes the proof.□

Appendix B. Details on global analysis

Proof of Theorem 1.

Using the Morse Lemma Verhulst (1996) page 19, the phase-plane Eq. (13) is obtained. Considering that $\varphi = (d\phi/dx)$ and $\gamma > 0$, by letting $k = 2H(\phi_j, 0) + (c^2/\gamma)$, it can be seen that the approximate solution (14) satisfies equation (13).□

Proof of Theorem 2.

Let $\rho(\phi, \varphi)$ be a real valued function with continuous first order partial derivatives. Define the function $G : \mathbb{R}^2 \to \mathbb{R}^2$,

$$G(\phi, \varphi) = \frac{\partial}{\partial\phi}\left(\rho\frac{d\phi}{dx}\right) + \frac{\partial}{\partial\varphi}\left(\rho\frac{d\varphi}{dx}\right). \tag{B.1}$$

Denote ρ_ϕ and ρ_φ as partial derivatives of ρ with respect to ϕ and φ, then using the right-hand sides of both equations in (9), $G(\phi, \varphi)$ is written as,

$$G(\phi, \varphi) = \rho_\phi\varphi + \rho\frac{d\varphi}{d\phi} + \frac{1}{D_m}\rho_\varphi(d_m\phi - \epsilon b(\phi)(x)) + \frac{1}{D_m}\rho\left(d_m\frac{d\phi}{d\varphi} - \frac{\epsilon db(\phi(x))}{d\varphi}\right). \tag{B.2}$$

Let $X = \frac{d\varphi}{d\phi}$ and apply the chain rule for the last term in (B.2), we get that,

$$G(\phi, \varphi) = \rho_\phi\varphi + X(\rho + \rho_\varphi\varphi) + \frac{\rho}{D_m X}(d_m - \epsilon b'(\phi(x))). \tag{B.3}$$

Let $\rho(\phi, \varphi) = \varphi(d_m\phi - \epsilon b(\phi))$. Using (9) we can see that

$$X = \frac{d_m\phi - \epsilon b(\phi)}{D_m\varphi} = \frac{\rho}{D_m\varphi^2}.$$

Hence expression (B.3) takes the form

$$G(\phi, \varphi) = 2\varphi^2(d_m - \epsilon b'(\phi)) + 2\frac{\rho^2}{D_m\varphi^2} + \varphi^2(d_m - \epsilon b'(\phi)) > 0. \tag{B.4}$$

Using Dulac's criterion Verhulst (1996), the proof is complete.□

Proof of Theorem 4

By Theorem 3 part *(i)*, the trivial solution $w = 0$ of (4) is locally asymptotically stable when $b'(0) < d_m/\epsilon$.

When $D_m = 0$, $D_l = 0$ (and therefore $\alpha = 0$) Eq. (4) is reduced to

$$\frac{dw(t)}{dt} = -d_m w(t) + \epsilon b(w(t - \tau)). \tag{B.5}$$

From $0 < b(w(t)) \leq b'(0)w(t)$ for all $t > -\tau$, we get that $w'(t) \leq -d_m w(t) + \epsilon b'(0)w(t - \tau)$. Since the delay term has a positive coefficient, by a comparison argument Smith (1995) it is enough to show that solutions of

$$w'(t) = -d_m w(t) + \epsilon b'(0)w(t - \tau) \tag{B.6}$$

approach zero. Since we have $b'(0) < d_m/\epsilon$, in equation (B.6) the term delay has a smaller coefficient than the term without the delay. Hence, by Section 2 of Theorem 2.1 on page 70 of Kuang (1993), all solutions $w(t)$ of (B.6) converge to zero. This completes the proof.□

Proof of Theorem 5

Part (i)

Let $b(\phi) = b_4(\phi)$. The equilibrium ϕ_2 exists under the condition $\frac{\epsilon p}{d_m} > ae$. the phase path corresponding to the Eq. (9) is given by

$$\varphi(\phi) = \pm\sqrt{2}(s_4 - V_4(\phi))^{\frac{1}{2}}, \tag{B.7}$$

where

$$\begin{aligned} V_4(\phi) &= \frac{1}{D_m}\left(-d_m\int \phi d\phi + \epsilon p\int \phi^2 e^{-a\phi}d\phi\right), \\ &= \frac{-1}{D_m}\left(\frac{d_m}{2}\phi^2 + \frac{\epsilon p}{a}\left(\phi^2 + \frac{2}{a}\phi + \frac{2}{a^2}\right)e^{-a\phi}\right). \end{aligned} \tag{B.8}$$

Let $s_4 = -(2\epsilon p/a^3 D_m)$ then $\varphi(\phi_1) = 0$, where $\phi_1 = 0$. Note that ϕ_1 and ϕ_3 are saddles, while ϕ_2 is a center. Hence $|\varphi(\phi)|$ has minimum values at ϕ_1 and ϕ_3 and has a maximum value at ϕ_2. It can be shown that $s_4 - V_4(\phi)$ increases for $0 < \phi < \phi_2$ and it decreases for $\phi_2 < \phi < \phi_3$. Since $V_4(\phi_3) = 0$, there must be a point $\phi^* \in (\phi_2, \phi_3)$, such that $s_4 - V_4(\phi^*) = 0$. Hence, by the continuity and the symmetry of (B.7), the homoclinic orbit is defined by the Eq. (B.7) for $\phi \in [0, \phi^*]$.

Part (ii)

Let $b(\phi) = b_5(\phi)$. The equilibrium ϕ_2 exists under the condition $\frac{\epsilon p}{d_m} > a$. Similar to the previous proof,

$$\varphi(\phi) = \pm\sqrt{2}(s_5 - V_5(\phi))^{\frac{1}{2}}, \tag{B.9}$$

where s_5 is a constant and V_5 is obtained as follows,

$$\begin{aligned} V_5(\phi) &= \frac{1}{D_m}\left(-d_m\int \phi d\phi + \epsilon p\int \frac{\phi^2}{1+a\phi}d\phi\right) \\ &= \frac{1}{D_m}\left(\frac{-d_m}{2}\phi^2 + \frac{\epsilon p}{2a^3}(a\phi)(a\phi - 2) + 2\ln|1+a\phi|\right). \end{aligned} \tag{B.10}$$

Let $s_5 = 0$, then $(\phi_1, \varphi(\phi_1)) = (0, 0)$. Since ϕ_1 and ϕ_2 are the only extrema of $\varphi(\phi)$ and $\varphi(\phi)$ is symmetric with respect to the ϕ axis, the same argument is applied here and there exists a homoclinic orbit connecting ϕ_1 to itself.

The proof of part (iii) is similar to that of part (i) and is omitted.□

Proof of Theorem 6

When $b_4(\phi)$ is considered by choosing $s_4 = -\frac{2\epsilon p}{a^3 D_m}$ we have $\varphi(\phi_1)) = 0$ (see proof of Theorem 5 part (i)). We only need to show that $\varphi(\phi_3) = 0$. Let

$$\frac{\epsilon p}{d_m} = \frac{ae^k}{k}, \tag{B.11}$$

for $k > 1$; then

$$\phi_3 = \frac{k}{a}. \tag{B.12}$$

Substituting (B.11) and (B.12) into $\frac{1}{2}(\varphi(\phi_3))^2$ we get that,

$$\begin{aligned} s_4 - V_4(\phi_3) &= \frac{d_m}{D_m} \\ &\quad\times\left(-\frac{2\epsilon p}{a^3 d_m} + \frac{k^2}{2a^2} + \frac{\epsilon p}{ad_m}\left(\frac{k^2+2k+2}{a^2}\right)e^{-k}\right), \\ &= \frac{d_m}{D_m a^2}\left(-\frac{2e^k}{k} + \frac{k^2}{2} + k + 2 + \frac{2}{k}\right), \end{aligned} \tag{B.13}$$

which has the root $r \approx 1.451$. Thus, for $\phi_3 = \frac{r}{a}$ we have $s_4 - V_4(\phi_3) = 0$, which gives rise to $\varphi(\phi_3) = 0$. It implies that ϕ_1 is connected to ϕ_3, when $\frac{\epsilon p}{d_m} = \frac{e^r}{r}a$.

When b_6 is considered we have,

$$\varphi(\phi) = \pm\sqrt{2}(s_6 - V_6(\phi))^{\frac{1}{2}},$$

where $V_6(\phi)$ is obtained as follows,

$$\begin{aligned} V_6(\phi) &= \frac{1}{D_m}\left(-d_m\int \phi d\phi + \epsilon p\int \frac{\phi^2 d\phi}{(1+a\phi)^2}\right), \\ &= \frac{1}{D_m} \\ &\quad\times\left(-d_m\phi^2 + \frac{\epsilon p}{a^3}\left(1 + a\phi - \frac{1}{1+a\phi} - 2\ln|1+a\phi|\right)\right). \end{aligned} \tag{B.14}$$

Let $s_6 = 0$, then $(\phi_1, \varphi(\phi_1)) = (0, 0)$. Then we are required to have $\varphi(\phi_3) = 0$.

Noting that $\phi_3 > \frac{1}{a}$, there exists $k > 1$ such that $\phi_3 = \frac{k}{a}$. Then we have $\frac{\epsilon p}{d_m} = \frac{a(1+k)^2}{k}$. Similar to the procedure above we get that,

$$\begin{aligned} s_6 - V_6(\phi_3) &= -\frac{d_m}{D_m} \\ &\quad\times\left(-\frac{k^2}{a^2} + \frac{\epsilon p}{d_m a^3}\left(1 + k - \frac{1}{1+k} - 2\ln(1+k)\right)\right) \\ &= \frac{-d_m}{kD_m a^2}\left(3k^2 + 2k - 2(1+k)^2\ln(1+k)\right), \end{aligned} \tag{B.15}$$

which is positive for all $k > 1$. Hence, there is no path connecting ϕ_1 to ϕ_3.□

Appendix C. Supplementary Data

Supplementary data associated with this article can be found, in the online version, at http://dx.doi.org/10.1016/j.ecocom.2014.10.007.

References

Allee, W.C., 1927. Animal aggregations. Quart. Rev. Biol. 2, 367–398.

Allee, W.C., 1933. Animal Aggregations. A Study in General Sociology Chicago Univ. Press, Chicago.

Anazawa, M., 2009. Bottom-up derivation of discrete-time population models with the Allee effect. Theor. Popul. Biol. 75 (1) 56–67.

Asmussen, M.A., 1979. Density-dependent selection II. Allee Effect. Am. Nat. 114, 796–809.

Aviles, L., 1999. Cooperation and non-linear dynamics: an ecological perspective on the evolution of sociality. Evol. Ecol. Res. 1, 459–477.

Bani-Yaghoub, M., Amundsen, D.E., 2014. Oscillatory traveling waves for a population diffusion model with two age classes and nonlocality induced by maturation delay. Comput. Appl. Math., http://dx.doi.org/10.1007/s40314-014-0118-y.

Britton, N.F., 1989. Aggregation and the competitive exclusion principle. J. Theor. Biol. 136 (1) 57–66.

Britton, N.F., 1990. Spatial structures and periodic travelling waves in an integro-differential reaction-diffusion population model. SIAM J. Appl. Math. 50 (6) 1663–1688.

Beverton, R.J.H., Holt, S.J., 1957. On the dynamics of exploited fish populations. Fisheries Investigations Series II, 19. H. M. Stationery Office, London.

Boukal, D.S., Berec, L., 2002. Single-species models of the Allee effect: extinction boundaries, sex ratios and mate encounters. J. Theor. Biol. 218, 375–394.

Dennis, B., 1989. Allee effects: population growth, critical density, and the chance of extinction. Nat. Resour. Model. 3, 481–538.

Doedel, E.J., Friedman, M.J., 1989. Numerical computation of heteroclinic orbits. J. Comput. Appl. Math. 26, 155–170.

Eskola, H.T.M., Parvinen, K., 2007. On the mechanistic underpinning of discrete-time population models with Allee effect. Theor. Popul. Biol. 72, 41–51.

Faria, T., Huang, W., Wu, J., 2006. Traveling waves for delayed Reaction-Diffusion equations with global response. Proc. R. Soc. Lond. Ser. A Math. Phys. Eng. Sci. 462 (2065) 229–261.

Friedman, J., Doedel, E.J., 1991. Numerical computation and continuation of invariant manifolds connecting fixed points. SIAM J. Numer. Anal. 28, 789–808.

Györi, I., Ladas, G.E., 1991. Oscillation Theory of Delay Differential Equations: With Applications. Oxford University Press, Clarendon ISBN 978-0198535829.

Gopalsamy, K., 1992. Stability and Oscillations in Delay Differential Equations of Population Dynamics. Kluwer Academic Publishers, Dordrecht, The Netherlands.

Gourley, S.A., So, J.W.H., Wu, J.H., 2004. Nonlocality of reaction-diffusion equations induced by delay: biological modeling and nonlinear dynamics. J. Math. Sci. 124 (4) 5119–5153.

Guckenheimer, J., Holmes, P., 1983. Nonlinear Oscillations, Dynamical Systems, and Bifurcations of Vector Fields. Springer-Verlag, New York.
Gurney, W.S.C., Blythe, S.P., Nisbet, R.M., 1980. Nicholson's blowflies revisited. Nature 287, 17–21.
Jordan, D.W., Smith, P., 1999. Nonlinear Ordinary Differential Equations: An Introduction to Dynamical Systems. Oxford University Press, Oxford.
Kuang, Y., 1993. Delay Differential Equations with Applications in Population Dynamics. Academic Press, Inc., San Diego.
Li, W.-T., Ruan, S., Wang, Z.-C., 2007. On the diffusive Nicholson's blowflies equation with nonlocal delay. J. Nonlinear Sci. 17, 505–525.
Liang, D., Wu, J., 2003. Travelling waves and numerical approximations in a reaction advection diffusion equation with nonlocal delayed effects. J. Nonlinear Sci. 13, 289–310.
Liang, D., Wu, J., Zhang, F., 2005. Modelling population growth with delayed nonlocal reaction in 2-dimensions. Math. Biosci. Eng. 2 (1) 111–132.
May, R.M., 1980. Mathematical models in whaling and fisheries management. In: Oster, G.F. (Ed.), Some Mathematical Questions in Biology. American Mathematical Society, Providence, RI, pp. 1–64.
McCarthy, M.A., 1997. The Allee effect, finding mates and theoretical models. Ecol. Model. 103, 99–102.
Memory, M.C., 1989. Bifurcation and asymptotic behaviour of solutions of a delay-differential equation with diffusion, SIAM. J. Math. Anal. 20, 533–546.
Metz, J.A.J., Diekmann, O., 1986. The Dynamics of Physiologically Structured Populations. Springer-Verlag, New York.
Nicholson, A.J., 1954. An outline of the dynamics of animal populations. Aust. J. Zool. 2, 9–65.
Nicholson, A.J., 1957. The self adjustment of populations to change. Cold Spring Harb. Symp. Quant. Biol. 22, 153–173.
Smith, H.L., 1995. Monotone Dynamical Systems: An Introduction to the Theory of Competitive and Cooperative Systems. American Mathematical Society ISBN-10: 082180393X.
Smith, H., Thieme, H., 1991. Strongly order preserving semiflows generated by functional differential equations. J. Differ. Equ. 93, 332–363.
So, J.W.-H., Yang, Y., 1998. Dirichlet problem for the diffusive Nicholson's blowflies equation. J. Differ. Equ. 150, 317–348.
So, J.W.-H., Wu, J., Yang, Y., 2000. Numerical Hopf bifurcation analysis on the diffusive Nicholson's blowflies equation. Appl. Math. Comput. 111, 53–69.
So, J.W.-H., Wu, J., Zou, X., 2001. A reaction-diffusion model for a single species with age-structure. I Traveling wavefronts on unbounded domains. Proc. R. Soc. Lond. A 457, 1841–1853.
So, J.W.-H., Zou, X., 2001. Travelling waves for the diffusive Nicholson's blowflies equation. Appl. Math. Comput. 122, 385–392.
Verhulst, F., 1996. Nonlinear Differential Equations and Dynamical Systems, Second. Springer-Verlag, Berlin.
Wells, H., Strauss, E.G., Rutter, M.A., Wells, P.H., 1998. Mate location, population growth and species extinction. Biol. Conserv. 86, 317–324.
Weng, P., Liang, D., Wu, J., 2008. Asymptotic patterns of a structured population diffusing in a two-dimensional strip. Nonlinear Anal. 69, 3931–3951.
Yadav, R.T., 2006. Environmental Biotechnology. Discovery Publishing House, Delhi.